Rod and cone pathway signaling and interaction under mesopic illumination

Andrew J. Zele
Institute of Health and Biomedical Innovation and School of Optometry and Vision Science, Queensland University of Technology, Brisbane, Australia.

Michelle L. Maynard
Institute of Health and Biomedical Innovation and School of Optometry and Vision Science, Queensland University of Technology, Brisbane, Australia.

Beatrix Feigl
Institute of Health and Biomedical Innovation and School of Biomedical Science, Queensland University of Technology, Brisbane, Australia
Queensland Eye Institute, Brisbane, Australia

This study investigates the time-course and post-receptoral pathway signaling of photoreceptor interactions when the rod (R) and three cone (L, M, S) photoreceptor classes contribute to mesopic vision. A four-primary photostimulator independently controls photoreceptor activity in human observers. The first experiment defines the temporal adaptation response of receptoral (L-, S-cone, rod) and post-receptoral (LMS, LMSR, +L-M) signaling and interactions. Here we show that nonopponent cone-cone interactions (L-cone, LMS, LMSR) have monophasic temporal response patterns whereas opponent signals (+L-M, S-cone) show biphasic response patterns with slower recovery. By comparison, rod-cone interactions with nonopponent signals have faster adaptation responses and reduced sensitivity loss whereas opponent rod-cone interactions are small or absent. Additionally, the rod-rod interaction differs from these interaction types and acts to increase rod sensitivity due to temporal summation but with a slower time course. The second experiment shows that the temporal profile of the rod signal alters the relative rod contributions to the three primary post-receptoral pathways. We demonstrate that rod signals generate luminance (+L+M) signals mediated via the MC pathway with all rod temporal profiles and chromatic signals (L/L+M, S/L+M) in both the PC and KC pathways with durations >75 ms. Thus, we propose that the change in relative weighting of rod signals within the post-receptoral pathways contributes to the sensitivity and temporal response of rod and cone pathway signaling and interactions.

Keywords: mesopic, temporal, adaptation, rod-cone interaction, post-receptoral

Citation: Zele, A. J., Maynard, M. L., & Feigl, B. (2013). Rod and cone pathway signaling and interaction under mesopic illumination. *Journal of Vision*, *13*(1):21, 1–19, http://www.journalofvision.org/content/13/1/21, doi:10.1167/13.1.21.

Introduction

Rod and cone photoreceptor signaling under mesopic illumination is multiplexed in post-receptoral neural pathways and this provides both a neurophysiological basis for interactions between the photoreceptor signals (Daw, Jensen, & Brunken, 1990; Lee, Martin, & Grünert, 2010; Polyak, 1948) and subserves interactions that alter mesopic visual function (Barbur & Konstantakopoulou, 2012; Buck, Juve, Wisner, & Concepcion, 2012; Cao & Lu, 2012; Feigl, Cao, Morris, & Zele, 2011; Zele, Kremers, & Feigl, 2012). Two illumination dependent pathways convey the rod signals to post-receptoral ON and OFF pathways. At mesopic and high scotopic illuminations, rod signals are transmitted to post-receptoral neurons through rod-cone gap junctions and ON and OFF cone bipolar cells and at low scotopic illuminations, rod signals are transmitted via rod bipolar, AII amacrine, and ON cone bipolar cells (Daw et al., 1990; Kolb & Famiglietti, 1974). The AII also mediates rod signaling to OFF cone bipolar cells in mammals (e.g., Li, Chen, & DeVries, 2010), but at this time it has not been demonstrated in primates (Lee et al., 2010). Physiological recordings have detected strong rod signals in the magnocellular (MC) pathway in macaque (Cao, Lee, & Sun, 2010; Lee, Smith, Pokorny, & Kremers, 1997; Virsu & Lee, 1983), rhesus (Wiesel & Hubel, 1966), and cat (Virsu, Lee, & Creutzfeldt, 1977), weak and variable rod signals in the parvocellular (PC) pathway of macaque (Lee, Pokorny, Smith, Martin, & Valberg,

doi: 10.1167/13.1.21 Received July 19, 2012; published January 16, 2013 ISSN 1534-7362 © 2013 ARVO

Downloaded from jov.arvojournals.org on 10/03/2022

1990; Lee et al., 1997; Purpura, Tranchina, Kaplan, & Shapley, 1990; Virsu & Lee, 1983) and marmoset (Weiss, Kremers, & Maurer, 1998), and rod signals in the koniocellular (KC) pathways of macaque (Crook et al., 2009; Field et al., 2009), although other studies have detected no or little input to KC in macaque (Lee et al., 1997) or rhesus (Wiesel & Hubel, 1966).

Crawford (1947) first demonstrated that multiple mechanisms operate on the tens to hundreds of millisecond timescale to mediate the transition to a steady state of adaptation following prolonged exposure to an illumination change. These illumination dependent changes in visual sensitivity (Stiles, 1978) are controlled by time-dependent adaptation processes (Adelson, 1982; Graham & Hood, 1992; Hecht, Haig, & Chase, 1937; Hood & Finkelstein, 1986; Kohn, 2007; Smith, Pokorny, Lee, & Dacey, 2008; Stockman, Langendörfer, Smithson, & Sharpe, 2006). The general observation with achromatic test stimuli measured under photopic illumination is that threshold increases prior to light onset (backward masking), reaching maximum threshold at onset (Baker, 1953; Bowen, Markell, & Schoon, 1980; Crawford, 1947; Hood, Ilves, Maurer, Wandell, & Buckingham, 1978; Poot, Snippe, & van Hateren, 1997; Zele & Vingrys, 2000), but there are reports of peak threshold elevations at 25 ms prior to light onset (Pokorny, Sun, & Smith, 2003) and at about 50 ms post light onset (Boynton, Bush, & Enoch, 1954). In the few studies of the time course of adaptation under low photopic, mesopic, and scotopic adaptation conditions, maximum threshold elevation is delayed by up to 50 ms after light onset (Adelson, 1982; Buck, 1985; Buck, Stefurak, Moss, & Regal, 1984; Frumkes, Sekuler, Barris, Reiss, & Chalupa, 1973; Hayhoe, Benimoff, & Hood, 1987; Limb & Tulunay-Keesey, 1981; von Wiegand, Hood, & Graham, 1995; White, Kelly, & Sturr, 1978; Zele & Vingrys, 2007), possibly reflecting differences in the temporal latency of rod and cone signaling (Gouras & Link, 1966). It is still to be determined how illumination dependent changes in the temporal visual response affect the psychophysically measured temporal response of photoreceptor signaling under mesopic light levels.

The early forms of the duplicity theory of vision (Müller, 1923; Nagel, 1911; Schultze, 1866; von Kries, 1929) postulated little or no interaction between signals originating in rods and cones, but it's now clear that rod and cone photoreceptor signals interact within shared retinal pathways (Polyak, 1948) and alter visual function and performance (for review, see Buck, 2004). A significant challenge is confronted when studying mesopic vision due to the change in temporal response of rod and cone signaling with wavelength, adaptation level, and/or retinal location, parameters that were historically varied in experiments to bias activity between rods and cones. With such experimental approaches, these stimulus dependent changes in rod and cone sensitivity confound the direct comparison of their temporal adaption responses, and in some cases, the comparison of results between studies.

Recent advances in instrumentation (Pokorny, Smithson, & Quinlan, 2004) have provided new opportunities for understanding and defining mesopic vision. The psychophysical analysis of rod contributions to color vision have defined the rod inputs to the inferred MC, PC, and KC pathways (Cao, Pokorny, & Smith, 2005; Cao, Pokorny, Smith, & Zele, 2008; Cao, Zele, & Pokorny, 2008) and show for temporal processing that rod and cone signal interactions decrease the temporal bandwidth of cone pathways (Zele, Cao, & Pokorny, 2008) and attenuate the critical fusion frequency (Cao & Lu, 2012; Cao, Zele, & Pokorny, 2006). The rod and cone interaction can occur within shared retinal pathways, or the photoreceptor signals can be processed independently (Kremers & Meierkord, 1999; Sun, Pokorny, & Smith, 2001b; Zele et al., 2012). At present there remain unresolved problems in the understanding of mesopic visual function and performance, of which this study uses a four-primary photostimulator to control the L-, M-, and S-cone and rod photoreceptor excitations at the same chromaticity and mesopic adaptation level to infer the neural substrates mediating the photoreceptor interactions (Pokorny et al., 2004). The first experiment determines the adaptation response of cone signaling, rod signaling, and rod and cone signaling when temporally filtered by the anatomically and physiologically well-defined ON-pathway of the MC, PC, and KC pathways. A second experiment defines the post-receptoral pathway temporal filtering of rod signals. Together the experiments identify the amplitude and timing of the temporal adaptation response of the interaction between the rod and cone signaling in the ON-pathway and identify the signature post-receptoral pathways mediating the rod signal.

Methods

Observers

Two female participants, O_1 (female, age 35 years) and O_2 (female, age 27 years) served as observers. One observer (O_2) was naïve to the purpose of the experiment and was allowed sufficient practice sessions before experimentation began. Both had normal visual acuity (6/6) measured by the Bailey-Lovie visual acuity chart and were normal trichromats as assessed with Farnsworth D-15 and Ishihara pseudochromatic plates. Intraocular pressures were normal and no opacities were noted on the crystalline lens based on the AREDS

Downloaded from jov.arvojournals.org on 10/03/2022

grading system. Fundus examination revealed no ocular pathology.

Apparatus

Excitation of the four photoreceptor types in the retina was independently controlled (Shapiro, Pokorny, & Smith, 1996) using a two-channel, four-primary photostimulator with eight primary lights, four for the central field and four for the surround field (Pokorny et al., 2004). The narrow-band primaries were generated using light-emitting diodes (LEDs) and narrow-band interference filter combinations with peak wavelengths at 459 nm (blue), 516 nm (cyan), 561 nm (green), and 658 nm (red). The LED levels were controlled by amplitude modulation of a 20 kHz carrier inputting an eight analog output channel Dolby soundcard (M-Audio-Revolution 7.1 PCI) (Puts, Pokorny, Quinlan, & Glennie, 2005) with a 24 bit digital-to-analog (D/A) converter operating at a 192 kHz sampling rate and electronic drivers that include custom built demodulators and voltage-to-frequency converters to provide 1-μs pulses at frequencies up to 250 kHz (Swanson, Ueno, Smith, & Pokorny, 1987). This system has a precision of greater than 16 bits (Puts et al., 2005). Custom developed software controlled the stimuli using an Apple Macintosh G5 computer. A precision digital scopemeter (Fluke model 124, Netherlands) confirmed the stimulus timings. Examples of the photostimulator implementation are given elsewhere (Cao, Zele, et al., 2008; Zele et al., 2008; Zele et al., 2012).

Calibration

The calibration involved two steps, a physical light calibration and an individual observer calibration. The physical light measurements were of the LED spectral output and for the voltage-illuminance linearization (Pokorny et al., 2004; Sun, Pokorny, & Smith, 2001a). The observer calibrations corrected for differences in prereceptoral filtering (i.e., lens and macular pigment) and receptoral spectral sensitivities between the individual observers and the 1964 10° standard observer. The theoretical match of the International Commission on Illumination (CIE) (1964) 10° standard observer for the mixture of the 459 nm and 561 nm primaries and the mixture of 516 nm and 658 nm was calculated using the mean CIE (1964) 10° color matching functions. The differences in prereceptoral filtering were determined by comparing the theoretical values of the 10° standard observer with the relative radiances of the four lights required by the individual observer to complete a photopic color match. The photopic color match required the observer to equate two successively presented primary light combinations (516 and 658 nm matched to 459 and 561 nm; the 561 nm primary is the reference light) by adjusting the combined luminance and the ratio of the 516 and 658 nm primaries and the luminance of the 459 nm primary. This color match was conducted by each observer at the same peripheral retinal location of the stimulus field as for the experiments (7° eccentricity). Further details of the observer calibration procedures are described elsewhere (Cao et al., 2005; Cao, Zele, & Pokorny, 2007; Pokorny et al., 2004; Sun et al., 2001a).

Two independent tests confirmed the observer calibration and rod isolation. In the first control procedure, the color appearance of an incremental rod signal was greenish-blue and brighter, consistent with published reports (Buck, Knight, Fowler, & Hunt, 1998; Lie, 1963; Nagel, 1924; Pokorny, Lutze, Cao, & Zele, 2006; Stabell & Stabell, 1971; Trezona, 1970; Willmer, 1950). This rod color percept for a 1 Hz, 30% rod pedestal (constant cone excitation) is equivalent to a decrease in L/(L+M), increase in S/(L+M) and increase in (L+M), consistent with published reports (Cao et al., 2005; Cao, Pokorny, et al., 2008; Cao, Zele, et al., 2008) (see Experiment 2). In the second control procedure, rod isolation was confirmed when an incremental rod pulse (30% rod contrast; constant cone excitation) that was highly conspicuous after dark adaptation was invisible for $\sim$ 4–5 minutes following extinction of the bleaching light.

Psychophysical paradigms

The test stimulus was presented in a 2° circular field centered within a 13° surround. The mean adaptation level of the field (5 Td) was metameric to an equal energy white (EEW) spectrum. A white fixation point located at 7° ensured observer stability when fixating eccentrically (Figure 1). In this center-surround stimulus configuration, the 13° surround was unmodulated and set the adaptation level; the test probe and conditioning pulse were presented in the center field (see next section). Between trials, the center and surround fields were equiluminant and produced a single uniform field (13° diameter). This stimulus setup examines local, within the stimulus area interactions, as compared to lateral interactions across the surround and center field (Cao et al., 2006; Goldberg, Frumkes, & Nygaard, 1983).

The test stimuli were specified in a relative cone Troland chromaticity space (Smith & Pokorny, 1996), which is the physiological cone excitation space of MacLeod and Boynton (1979) with the equal-energy-spectrum light normalized to 1.0 for S/(L+M). The CIE 10° color matching data were transformed to the cone based chromaticity space by applying the Smith and

Downloaded from jov.arvojournals.org on 10/03/2022

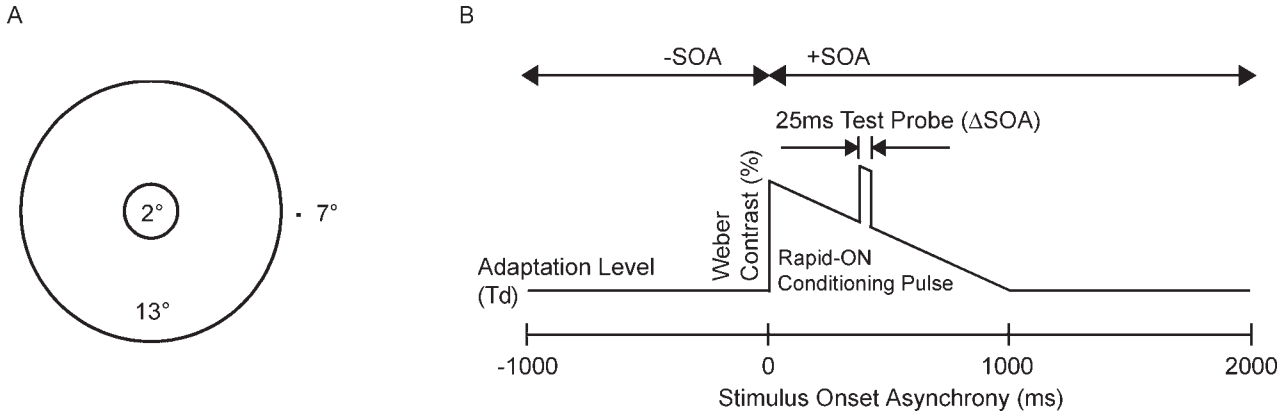

Figure 1. (A) Spatial configuration of the test stimulus. The test probe and conditioning pulse were presented in a 2° circular stimulus field set in a 13° surround (local stimulus interactions). The fixation point located the center of the 2° field at 7° eccentricity in the temporal retina. (B) Temporal configuration of the stimulus onset asynchrony (SOA) paradigm. Thresholds were measured for a 25 ms test probe as a function of the onset time (ΔSOA) of a 1000 ms rapid-ON sawtooth conditioning pulse (30% Weber contrast). The schematic shows one stimulus presentation. The time average retinal illuminance of the baseline chromaticities of the center and surround fields at the adaptation level was 5 photopic Td and metameric to the equal energy spectrum (SMLR = 5, 1.667, 3.333, 5 Td).

Pokorny (1975) transformation to the 1964 10° color matching functions (Shapiro et al., 1996). The notations adopted for the photoreceptor excitations were L (long wavelength sensitive cone), M (medium wavelength sensitive cone), S (short wavelength sensitive cone), and R (rod). Test stimulus photoreceptor excitations were then defined as combinations of the LMSR notation (e.g., R, S, +L-M, LMSR, LMS) with the excitation(s) of the unspecified photoreceptor type(s) being constant before, during, and after the stimulus presentations.

Experiment 1: Time-course of photoreceptor interactions

A stimulus onset asynchrony (SOA) paradigm (Crawford, 1947) determined the temporal adaptation response of photoreceptor interactions localized to the area of the 2° stimulus field (local photoreceptor interaction). Three photoreceptor combinations were investigated (cone-cone; rod-cone; rod-rod) with the stimulus selection based on the inferred post-receptoral pathways mediating the photoreceptor signals (MC: LMS, LMSR, and L-cone stimulus excitation; PC: +L-M; KC: S-cone stimulus excitation) (Cao et al., 2006). The L-cone signal inputs both +L+M and +L-M mechanisms and we infer mediation of this L-cone stimulus excitation may be via the nonopponent (luminance) pathway because it generates an increase in L-cone illuminance above the adapting background and there is commonality in the pattern of temporal responses to the L-cone excitation and the +L+M signaling under mesopic illumination (Cao et al., 2006). We use the term nonopponent for stimuli with LMS, LMSR, and L-cone excitations and opponent for the stimuli with +L-M and S-cone excitations.

The rectangular test probe was presented at predetermined SOAs relative to onset of a 1000 ms rapid-ON sawtooth conditioning pulse (Figure 1). A minimum 1000 ms trail time after conditioning pulse offset ensured adaptation to the conditioning pulse was complete before the next stimulus presentation. Note that in Crawford (1947) terminology, the conditioning pulse is labeled the conditioning field. Pilot studies were conducted to determine optimal stimulus duration, adaptation level, and conditioning pulse contrast for the experimental conditions. The test probe duration was 25 ms for the L-cone, LMS, LMSR, +L-M, and rod (R) excitation conditions and increased to 50 ms for the S-cone excitation condition so thresholds could be measured within the photostimulator gamut; the short probe duration should introduce no, or very little, change in adaptation. The conditioning pulse was 30% Weber contrast for the L-cone, S-cone, LMS, LMSR, and rod (R) excitation conditions and 13% for +L-M excitation condition so that threshold changes produced by the conditioning pulse were measurable within the photostimulator gamut. For all conditions, the 1000 ms conditioning pulse was visible, consistent with published data that show that stimuli with shorter durations than the integration period of the detection mechanism (i.e., the test probes used in these experiments) have higher thresholds than those for longer duration stimuli (i.e., a 1000 ms conditioning ramp) (Swanson, Pan, & Lee, 2008).

Eleven conditioning pulse (cp) and test probe (tp) stimulus combinations were studied across three photoreceptor excitation combinations. This included five $CONE_{cp}$:$CONE_{tp}$ excitation conditions (L:L-cone,

Downloaded from jov.arvojournals.org on 10/03/2022

LMS:LMS, LMSR:LMSR, +L-M:+L-M; S:S), five ROD_{cp}:$CONE_{tp}$ excitations (R:L, R:LMS, R:LMSR, R:+L-M, R:S), and one ROD_{cp}:ROD_{tp} excitation condition (R:R). The SOAs ranged from −500 ms (prior to conditioning pulse onset) to 1500 ms (500 ms post-conditioning pulse offset). The first observer (O_1) collected 12 SOAs for each condition and the second observer (O_2) sampled at a reduced number of SOAs (nine) to verify the major observations.

Four subconditions were completed by one observer (O_1). The first examined the effect of the temporal profile of the conditioning pulse ramp for the +L-M and S-cone photoreceptor excitations (i.e., slow-ON and rapid-ON sawtooth stimuli). The second, third, and fourth conditions examined the rod-rod interaction; the second condition studied the effect of the rod rapid-ON sawtooth conditioning pulse contrast on the threshold for the synchronously presented rod test probe (i.e., threshold versus contrast function measured at 0 ms SOA), and the third condition measured the temporal response to a rectangular rod decrement test probe as a function of the SOA relative to the onset of the rod rapid-ON sawtooth conditioning pulse. The fourth condition used a spatially larger 13° conditioning pulse to examine the effect of the spatial extent of the increment-increment rod-rod interaction on its amplitude and timing. These data were sampled at four SOAs (−500 ms, 0 ms, 100 ms, and 600 ms).

Contrast thresholds were measured using a yes/no paradigm (20% catch trials) and double random alternating staircase procedure. The contrast of the second stimulus was offset from the first by 10%. On each trial the observer reported their response of seeing or not seeing the test probe by pressing one of two buttons on a gamepad. Threshold contrast was halved after two correct responses and increased to the previous correct response threshold after one incorrect response. Once the criterion step size of 0.01 log units was attained, the staircase procedure continued until 10 reversals occurred, after which the next predetermined SOA staircase commenced. The average of the last six values of each staircase in each repeat was defined as threshold ($\mu \pm SEM$). The order of the SOA was randomized to control for observer habituation or fatigue.

A yes/no methodology was used instead of a forced choice methodology due to the time requirements of the experiment. We included 20% catch trials that presented only the rapid-ON ramp conditioning pulse to estimate any shifts in an observer's internal "yes" criterion, thus retaining a key advantage of the forced-choice methodology. In each of the 11 experimental conditions the stimuli were presented on average 100 times per SOA with 12 SOAs per run completed by one observer (total of 792 runs and ~36,000 trials) and nine SOAs completed per run by the second observer (total of 594 runs and ~27,000 trials). The number of incorrect "yes" responses to a catch trial was determined and the percentage error per SOA run calculated. All conditions were completed in a randomized order, conducted on separate days, and all reported data were calculated based on a minimum of three repeats. The accepted error range was ≤7%. If the percentage error for a run exceeded 10%, a repeat run was completed. The number of runs with >7% incorrect "yes" responses to the catch trial were 93 runs for Observer 1 and 67 runs for Observer 2. This is equivalent to 93/792 runs (11.7%) for one observer and 67/594 runs (11.2%) for the second observer. In other words, only ~11% of runs had false positive rates between 7% and 10% (i.e., ~89% of runs had incorrect "yes" response rates <7%). No runs had more than 10% false positive responses. The results of this analysis are in accordance with Poot et al. (1997) who had approximately 84% correct responses to the catch trials using a yes/no methodology with their stimulus onset asynchrony paradigm. This analysis showed that with the use of a yes/no method with two concurrent staircases and catch trials, there were no systematic patterns to the false positive responses for any stimulus onset asynchronies, photoreceptor excitation combinations, repeat trials, or participants that would indicate the threshold data patterns were due to criterion changes and not from true sensitivity changes.

Experiment 2: Post-receptoral pathways mediating the rod signals

Rod inputs to the inferred MC, PC, and KC post-receptoral pathways were defined as a function of the rod temporal profile using a color matching paradigm that specified the cone excitations that perceptually match the rod signal (Cao et al., 2005; Cao, Pokorny, et al., 2008; Cao, Zele, et al., 2008). The rod or cone signals were modulated in the central 2° field and the rod and cone excitations in the surround field were constant (Figure 2). The observer's task was to alter the cone excitations ([L+M]; L/[L+M] and S/[L+M]) in the matching epoch (rod excitation unmodulated) by pressing specific buttons on a gamepad to match the color appearance of the 30% Weber contrast rod excitation in the stimulus epoch (cone excitations unmodulated). The observer freely toggled between the rod stimulus epoch and the cone matching epoch. The temporal profiles of the stimuli included incremental rectangular stimuli (30% contrast; 25 ms to 1000 ms) and a rapid-ON sawtooth stimulus (30% contrast; 1000 ms). The 25 ms rectangular pulse and 1000 ms rapid-ON sawtooth were equivalent to the test probe and conditioning pulse stimuli in Experiment 1. The 1000 ms interstimulus interval was long enough to

Downloaded from jov.arvojournals.org on 10/03/2022

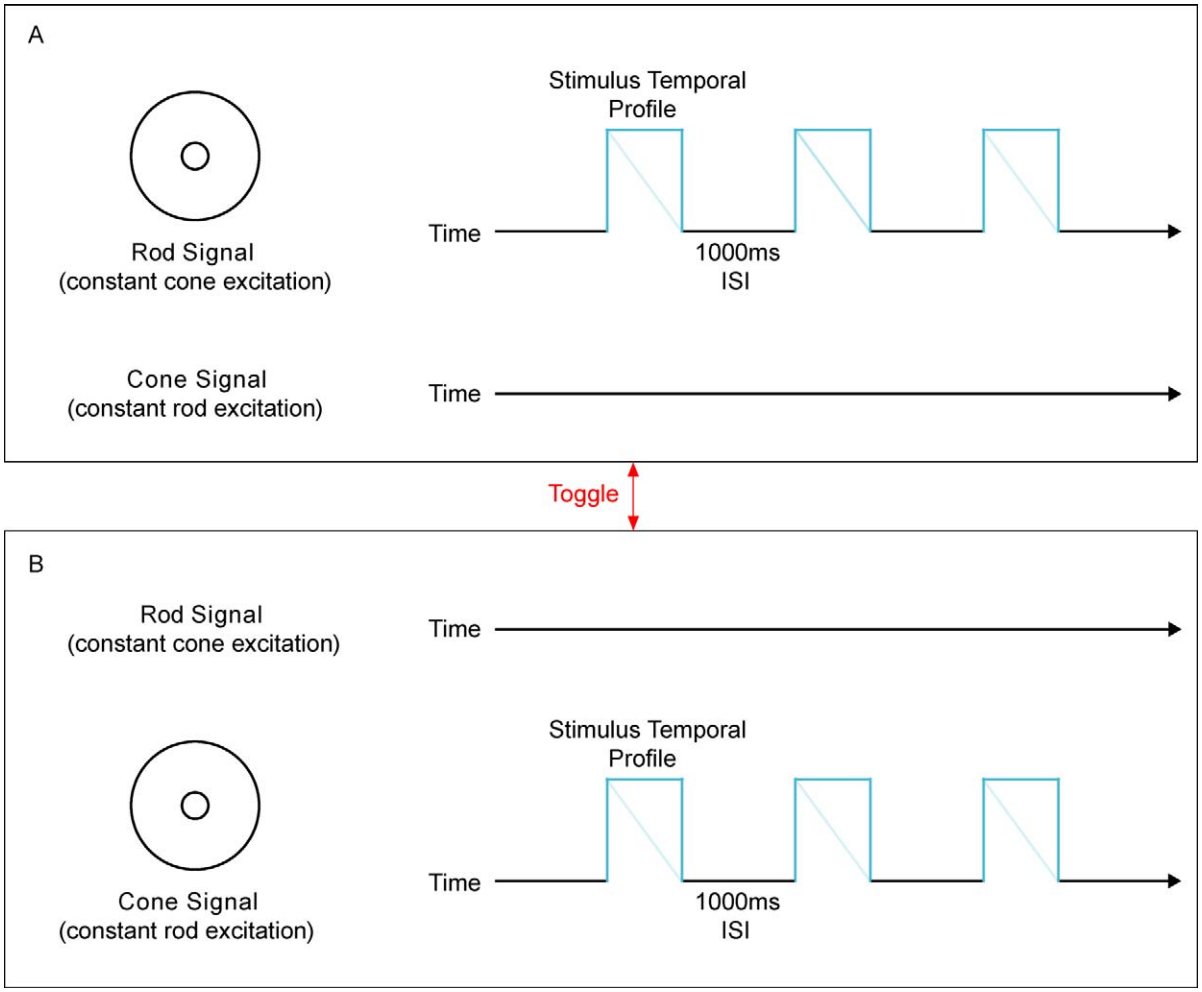

Figure 2. Temporal configuration of the rod color matching paradigm. (A) Rod stimulus signal epoch with constant cone excitation. (B) Cone matching epoch with constant rod excitation. The observer freely toggled between epochs (A and B). The observer's task was to match the 30% contrast rod signal (A) to a cone matching pedestal with the same stimulus temporal profile (B) by adjusting the cone excitations (L/[L+M]; S/[L+M]; L+M]). The surround rod and cone excitations were constant (SMLR = 5, 1.667, 3.333, 5 Td). The stimulus temporal profile included rectangular pulses (25 – 1000 ms; thick blue-green lines) and a 1000 ms rapid-ON sawtooth (thin blue-green lines). The rod stimulus and cone pedestal were perceptually indistinguishable at the color match.

avoid the perception of flicker and short enough to retain color memory (Nemes, Parry, & McKeefry, 2010; Rucci & Beck, 2005). When a satisfactory match was achieved, a button press confirmed the match and the process repeated. Seven conditions were investigated with a minimum of three repeats completed in at least four sessions for each condition. Condition orders were randomized. The mean and standard deviation were calculated for the repeats.

General procedure

Observers dark-adapted for 30 minutes prior to the beginning of data collection to ensure maximal rod sensitivity (Hecht, 1920). The duration of a single data session was then approximately 60 min. Dark adaptation and data collection were conducted in a light-tight room. For all measurements, observers aligned their right eye in Maxwellian view and a chin and forehead rest provided head position stability. The observers were well practiced before beginning the experiments.

Statistical analysis and modeling

A one-way analysis of variance (ANOVA) was conducted to examine the difference between mean contrast thresholds of each SOA for the eleven photoreceptor excitation conditioning pulse (cp) and test probe (tp) stimulus combinations, with $p < 0.05$ as significant (PASW Statistics 18, Hong Kong). Significant differences were evaluated using post-hoc t tests,

Downloaded from jov.arvojournals.org on 10/03/2022

controlling for familywise error using Fisher's least significant difference.

Weber contrast was calculated as a ratio of the test probe amplitude to the background adaptation level (background alone, or background and conditioning pulse). The SMLR Troland values of the background alone were 5, 1.667, 3.333, 5 Td prior to and after presentation of the conditioning pulse. The SMLR Troland level for the linearly decreasing conditioning pulse was determined at the time of each measurable SOA. When the test probe and conditioning pulse included the same photoreceptor excitations (e.g., S-S), the contrast calculation was referenced to the probe photoreceptor excitation (e.g., S) in the background (background alone, or background and conditioning pulse). For the rod-cone interaction condition, the data were always referenced to the photoreceptor excitation of the background.

The time-course was described by an exponential model fit to the data by minimizing the sum of squares differences between the model output and the data using the Excel solver routine. In this model

$$y = s * \exp(k * x) + r, (1)$$

y is the threshold, r is the resting level (%), k is the rate constant (ms^{-1}), and s is the span of change from minimum to maximum contrast (%). In the absence of a significant change in the temporal response, a straight line was fitted to the data (slope = 0).

Results

Experiment 1: Time-course of photoreceptor interactions

The data for the stimulus onset asynchrony paradigms for each experimental condition for the two observers are shown in Figures 3–7 (observer O_1, left panel; observer O_2, right panel). In the text, the data for observer O_2 is given in parentheses. In each figure, the Weber contrast (%) at test probe threshold is plotted as a function of its onset time (ms) relative to onset of the sawtooth conditioning pulse at time zero (0 ms). The error bars show standard errors of the mean ($\mu \pm SEM$) of at least three repeats for each condition. The solid lines in the figures represent the best fitting exponential functions. The photoreceptor excitation (LMS-cone and rod) for the conditioning pulse (cp) and test probe (tp) are defined by subscript. For example, LMS_{cp} LMS_{tp} represented an LMS-cone excitation of the conditioning pulse and test probe (both with constant rod excitation).

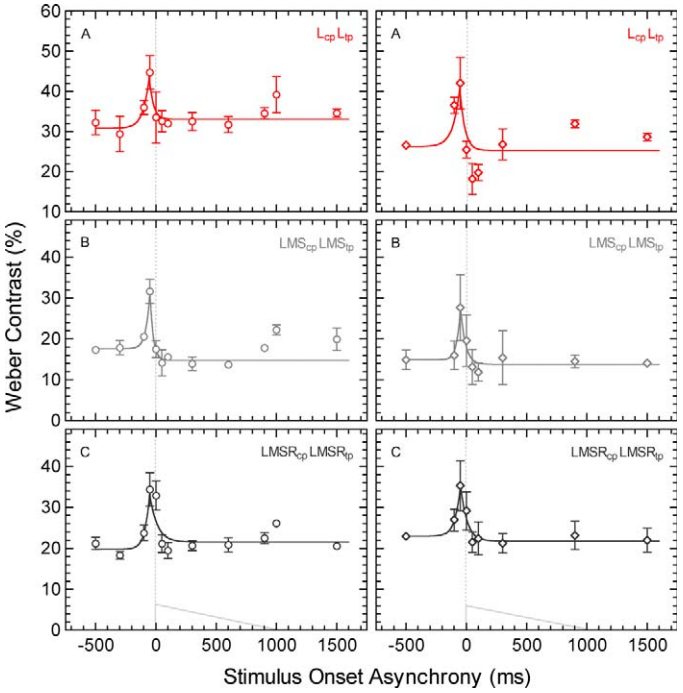

Figure 3. Time-course of interactions for L-cone, LMS, and LMSR signals (nonopponent cone-cone interactions). The panels in the left and right columns are for two observers (O_1, left panels; O_2, right panels). Panel A shows the Weber contrast threshold (%) for the 25 ms L-cone test probe (L_{tp}) measured as a function of the time to onset (stimulus onset asynchrony) of a 1000 ms rapid-ON sawtooth L-cone conditioning pulse (L_{cp}); the M-cone, S-cone, and rod excitation were constant. Panel B shows the time course of the LMS-cone interaction data; the rod excitation was constant ($LMS_{cp}LMS_{tp}$). Panel C shows the time course of the LMSR interaction data; all photoreceptors were modulated ($LMSR_{cp}LMSR_{tp}$). The rapid-ON sawtooth is schematically represented in Panel C as a grey line. The vertical grey line in all panels denotes the time of conditioning pulse onset (0 ms). The data show the mean and standard error. The lines show the best fitting exponential functions (Equation 1).

Cone-cone interactions

Figures 3A–C shows the Weber contrast thresholds for cone test probes (LMS, L-cone excitation) with constant rod excitation or with combined rod and cone excitation (LMSR). The threshold patterns showed monophasic responses. The threshold maximums occurred −50 ms prior to conditioning pulse onset and increased with an average time constant across the three conditions equal to 25.6 ± 6 ms^{-1} (24.9 ± 7 ms^{-1}). Contrast thresholds then decreased during presentation of the conditioning pulse period, returning to baseline within 50 ms after conditioning pulse onset and decreased with an average recovery time constant of 24.6 ± 8 ms^{-1} (22.5 ± 4 ms^{-1}). The baseline contrast thresholds were lowest for LMS excitation and highest for L-cone excitation. Although baseline thresholds for

Downloaded from jov.arvojournals.org on 10/03/2022

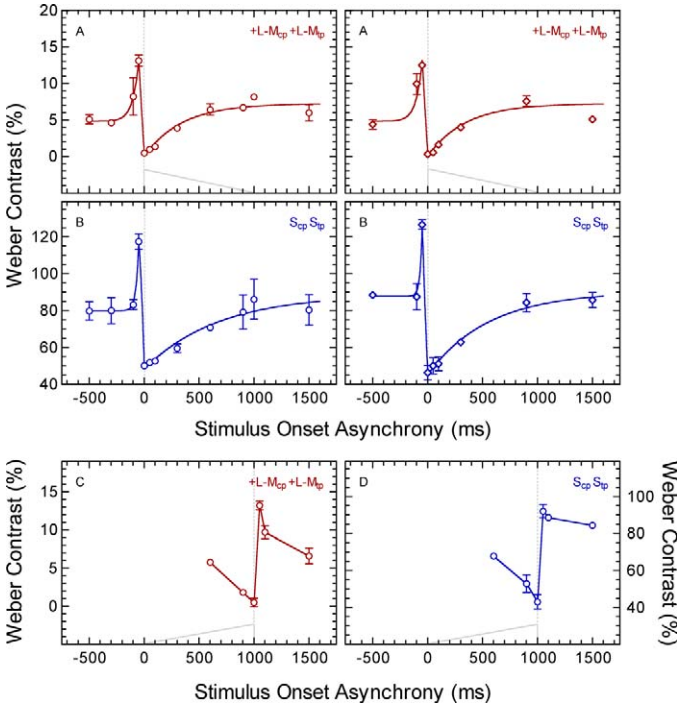

Figure 4. Time-course of interactions for +L-M and S-cone signals (opponent cone-cone interactions). Panel A shows the Weber contrast threshold (%) for the 25 ms +L-M test probe (+L-M_{tp}) measured as a function of the time to onset (stimulus onset asynchrony) of a 1000 ms rapid-ON sawtooth +L-M conditioning pulse (+L-M_{cp}); S-cone and rod excitation was constant. Panel B shows the time course of the S-cone interaction data (50 ms test probe); the L-cone, M-cone, and rod excitation were constant ($S_{cp}S_{tp}$). Panels A and B show the data for two observers (O_1, left panels; O_2, right panels) and Panels C and D show the data for one observer (O_1). Panel C shows the +L-M test probe threshold (+L-M_{tp}) measured as a function of the time to onset (stimulus onset asynchrony) of a 1000 ms slow-ON sawtooth +L-M conditioning pulse (+L-M_{cp}); S-cone and rod excitation were constant. Panel D shows the time course of the S-cone interaction data; the L-cone, M-cone, and rod excitation were constant ($S_{cp}S_{tp}$). The sawtooth conditioning pulses are schematically represented in Panels A, C, and D as grey lines. The data show the mean and standard error. The colored lines in Panels A and B show the best fitting exponential functions (Equation 1).

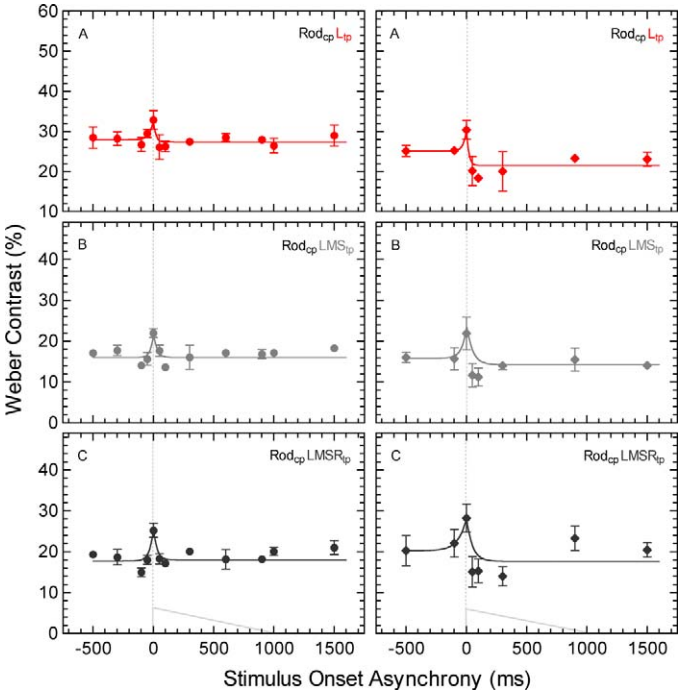

Figure 5. Time-course of interactions for rod and L-cone, LMS, and LMSR signals (nonopponent rod-cone interactions). The panels in the left and right columns are for two observers (O_1, left panels; O_2, right panels). Panel A shows the Weber contrast threshold (%) for the 25 ms L-cone test probe (L_{tp}) measured as a function of the time to onset (stimulus onset asynchrony) of a 1000 ms rapid-ON sawtooth rod conditioning pulse (Rod_{cp}). Panel B shows the time course of the LMS-cone test probe and rod conditioning pulse interaction data ($Rod_{cp}LMS_{tp}$). Panel C shows the time course of the LMSR test probe and rod conditioning pulse interaction data ($Rod_{cp}LMSR_{tp}$). The rapid-ON rod sawtooth is schematically represented in Panel C as a grey line. The vertical grey line in all panels denotes the time of conditioning pulse onset (0 ms). The data show the mean and standard error. The lines show the best fitting exponential functions (Equation 1).

LMSR excitation were ~4% higher than those for LMS excitation, this difference was not significant. There was a significant change in contrast threshold with SOA for observer O_1, $F(1, 11) = 16.08$, $p < 0.001$, and observer O_2, $F(1, 8) = 2.68$, $p = 0.039$, with post-hoc analysis demonstrating a significant difference between baseline and maximum threshold at −50 ms SOA for O_1 ($p < 0.001$) and O_2 ($p = 0.002$). Post-hoc analysis indicated the threshold increase at 1000 ms SOA for O_1 was not statistically significant from baseline (−500 ms SOA) in Figure 3A ($p = 0.284$), 3B ($p = 0.074$), or 3C ($p = 0.120$). The contrast threshold at 100 ms SOA for O_2 was not statistically significant from baseline (−500 ms SOA) in Figure 3A ($p = 0.058$), 3B ($p = 0.547$), or 3C ($p = 0.625$).

Figures 4A and 4B shows the Weber contrast thresholds for the +L-M and S-cone excitation with constant rod signals (+L-M_{cp}+L-M_{tp}; S_{cp} S_{tp}). The +L-M and S-cone data are biphasic; test probe threshold increased to maximum at −50 ms SOA and thereafter decreased rapidly to below baseline threshold. The minimum threshold was at conditioning pulse onset (0 ms SOA), followed by an increase in contrast threshold which returned to baseline by ~500 ms SOA. For the +L-M excitation, the time constant from baseline to the maximum threshold elevation was 18.0 ms^{-1} (12.0 ms^{-1}) and the recovery time constant from the minimum threshold to baseline was 2.9 ms^{-1} (3.0 ms^{-1}). For the S-cone excitation, the time constant to

Downloaded from jov.arvojournals.org on 10/03/2022

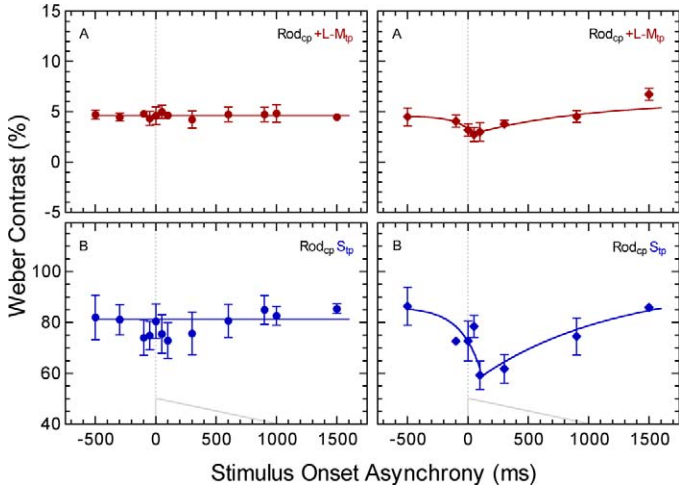

Figure 6. Time-course of interactions for rod and +L-M and S-cone signals (opponent rod-cone interactions). Panels A and B show the data for two observers (O_1, left panels; O_2, right panels). Panel A shows the Weber contrast threshold (%) for the 25 ms +L-M test probe (+L-M_{tp}) measured as a function of the time to onset (stimulus onset asynchrony) of a 1000 ms rapid-ON sawtooth rod conditioning pulse (Rod_{cp}). Panel B shows the threshold for the 50 ms S-cone test probe (S_{tp}) measured as a function of the time to onset of the rapid-ON sawtooth rod conditioning pulse (Rod_{cp}). The sawtooth conditioning pulses are schematically represented in Panels A and B as grey lines. The data show the mean and standard error. The colored lines in Panels A and B with the zero slopes indicate no significant interaction. Panel D shows the best fitting exponential functions (Equation 1).

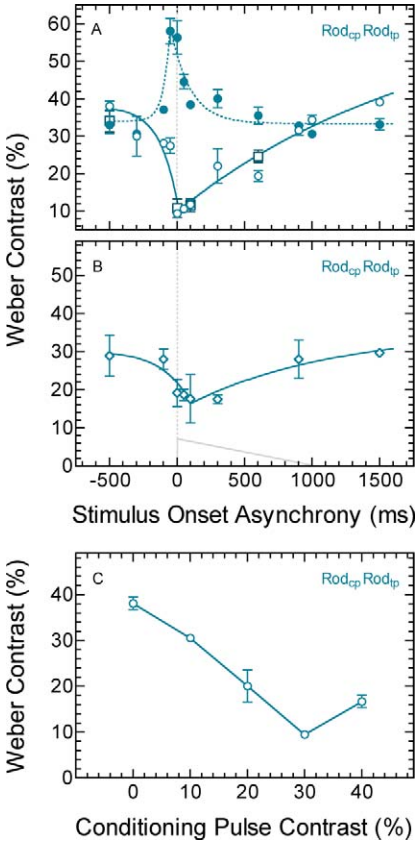

Figure 7. Time-course of interactions for rod signaling (rod-rod interactions). Panel A shows the data for observer O_1 (mean ± standard error). In this panel, the unfilled circles show thresholds for an incremental 25 ms, 2° rod test probe (Rod_{tp}) measured as a function of the time to onset (stimulus onset asynchrony) of a 1000 ms, 2° rapid-ON rod sawtooth conditioning pulse (Rod_{cp}); the L-cone, M-cone, S-cone excitation was constant. Filled circles in Panel A show the threshold for a decremental 25 ms rod test probe ($Rod_{tp}Rod_{cp}$). Unfilled squares show the threshold for the incremental 25 ms, 2° rod excitation measured as a function of the time to onset of a 1000 ms, 13° rapid-ON rod sawtooth conditioning pulse. Panel B shows the data for observer O_2 (mean ± standard error) with an incremental 25 ms rod test probe ($Rod_{tp}Rod_{cp}$). The sawtooth conditioning pulse is schematically represented in Panel B and the vertical grey lines denote the time of conditioning pulse onset (0 ms). The colored lines in Panels A and B show the best fitting exponential functions (Equation 1). Panel C shows Weber contrast threshold (%) of the incremental 25 ms rod test probe for observer O_1 measured as a function of the Weber contrast of the rod conditioning pulse (threshold versus contrast function); test probe thresholds were measured at 0 ms SOA. The data show the mean and standard error.

maximum threshold elevation was 48.0 ms^{-1} (50.0 ms^{-1}) and recovery time constant from the minimum threshold to baseline was 1.4 ms^{-1} (1.8 ms^{-1}). For the +L-M excitation, there was a significant change in contrast threshold with SOA for observer O_1, $F(1, 11) = 43.22$, $p < 0.001$, and observer O_2, $F(1, 8) = 11.71$, $p < 0.001$, with post-hoc analysis demonstrating significant differences between baseline and maximum threshold at −50 ms SOA for O_1 ($p < 0.001$) and O_2 ($p < 0.001$) and between maximum and minimum threshold at 0 ms SOA for O_1 ($p < 0.001$) and O_2 ($p = 0.021$). Similarly for the S-cone excitation, there was a significant change in contrast threshold for O_1, $F(1, 11) = 43.22$, $p < 0.001$, and O_2 $F(1, 8) = 11.71$, $p < 0.001$, with post-hoc analysis demonstrating significant differences between baseline and maximum threshold at −50 ms SOA for O_1 ($p < 0.001$) and O_2 ($p < 0.001$) and between maximum and minimum threshold at 0 ms SOA for O_1 ($p < 0.001$) and O_2 ($p < 0.03$).

To examine the effect of the sawtooth polarity on the time course of the adaptation response, Figures 4C and 4D show the SOA data for a slow-ON +L-M and S-cone sawtooth stimulus excitations. Both panels show the SOA data for one observer (O_1). The data for the +L-M and S-cone excitations were biphasic at conditioning pulse offset; the minimum threshold was coincident with conditioning pulse offset (1000 ms SOA) and the maximum threshold elevation was 50 ms after conditioning pulse offset (1050 ms SOA). The data measured with the slow-ON sawtooth in Figure

Downloaded from jov.arvojournals.org on 10/03/2022

4C and 4D are phase reversed with reference to the data measured with the rapid-ON sawtooth in Figures 4A and 4B.

Rod-cone interactions

The data reported in this section show the time-course of the change in threshold for a cone test probe excitation measured in the presence of a rapid-ON conditioning pulse that increases the rod excitation (constant cone excitations). Figure 5 shows the temporal adaptation response for L-cone, LMS, and LMSR photoreceptor excitations. The threshold patterns were monophasic; threshold maximums were synchronous with rod conditioning pulse onset (0 ms SOA) and the average time constant of the threshold elevation across the three conditions was equal to 26.9 ± 6 ms^{-1} (26.5 ± 8 ms^{-1}). Contrast thresholds then decrease during the conditioning pulse period and returned to baseline within 50 ms with an average recovery time constant of 39.0 ± 4.0ms^{-1} (31.6 ± 9.8 ms^{-1}). The baseline thresholds for the L-cone, LMS, and LMSR excitations were different, consistent with those for the cone-cone condition [L > LMSR > LMS] (Figure 3). The contrast threshold change from baseline to maximum threshold at 0 ms SOA was significant for observer O_1, $F(1, 11) = 11.82$, $p < 0.001$, and observer O_2, $F(1, 8) = 6.86$, $p < 0.001$, with post-hoc analysis demonstrating a significant difference between baseline and maximum threshold at 0 ms SOA for O_1 ($p < 0.001$) and O_2 ($p < 0.001$). The contrast threshold at 100 ms SOA for O_2 was statistically significant from baseline (−500 ms SOA) in Figure 5A ($p = 0.033$) but not significant in Figure 5B ($p = 0.07$) or 5C ($p = 0.061$).

Figure 6 shows the temporal adaptation response of cone-opponent test probes (+L-M, S-cone) during the presentation of a rapid-ON rod conditioning pulse. The interaction between the +L-M test probe excitation and the rod conditioning pulse with constant cone excitation (Figure 6A) was not significant for observer O_1, $F(1, 11) = 0.40$, $p = 0.944$, but showed a significant decrease in threshold during conditioning pulse presentation for observer O_2, $F(1,8) = 5.09$, $p = 0.004$, with a time constant of 7.9 ms^{-1} from baseline to the minimum threshold at 50 ms and a time course of recovery of 1.0 ms^{-1} during the conditioning pulse presentation. Post-hoc analyses demonstrated a significant difference between baseline threshold and minimum threshold ($p = 0.006$). The interaction between the S-cone test probe excitation and the rod conditioning pulse (Figure 6B) was not significant for observer O_1, $F(1, 11) = 1.25$, $p = 0.312$, but showed a significant decrease in threshold during the conditioning pulse presentation for observer O_2, $F(1, 8) = 10.05$, $p < 0.001$, with post-hoc analyses demonstrating a significant difference between baseline threshold and minimum threshold at 100 ms ($p = 0.012$). The time constant for the change in threshold from baseline to the threshold minimum at 100 ms was 5.8 ms^{-1} and then recovered to baseline at 0.9 ms^{-1}.

Rod-rod interactions

Figures 7A and 7B show the time-course of the Rod_{cp} Rod_{tp} interaction condition with constant LMS cone excitation. The rod increment conditioning pulse excitation and rod increment probe excitation data for observer O_1 (unfilled symbols in Panel A) and observer O_2 (Panel B) showed a monophasic threshold pattern opposite to that found for the cone-cone interaction data (Figure 3); the rod incremental probe threshold decreased prior to onset of the rod rapid-ON sawtooth conditioning pulse ($\tau = 7.5$ ms^{-1} [5.0 ms^{-1}]) and to a minimum threshold at 0 ms (100 ms), returning to baseline threshold within 1000 ms, with a recovery time constant of 0.5 ms^{-1} (0.9 ms^{-1}). There was a significant change in contrast threshold with SOA for observer O_1, $F(1, 11) = 52.71$, $p < 0.001$, and observer O_2, $F(1, 8) = 5.97$, $p = 0.002$, with post-hoc analysis demonstrating a significant difference between baseline and minimum threshold at 0 ms SOA for O_1 ($p < 0.001$) and at 100 ms for O_2 ($p = 0.003$). The threshold for the 2° incremental rod excitation measured in the presence of a spatially larger 13° rod conditioning pulse (square symbols in Figure 7A) showed a similar amplitude and time-course to that measured with the spatially coextensive 2° conditioning pulse (unfilled circles).

Figure 7A (filled symbols) shows the time-course of rod decrement probe excitation thresholds measured as a function of the time relative to the onset of the rod rapid-ON sawtooth conditioning pulse excitation (observer O_1). The monophasic pattern showed an increase in the rod decrement probe threshold prior to conditioning pulse onset ($\tau = 15.7$ ms^{-1}) with the maximum threshold at −50 ms. The contrast threshold then decreased during presentation of the conditioning pulse period, returning to baseline within 500 ms, with a recovery time constant of 6.9 ms^{-1}. Figure 7C shows the 25 ms rod incremental test probe threshold measured as a function of the contrast of the rod rapid-ON sawtooth conditioning pulse (1000 ms) and presented synchronously (0 ms SOA). This threshold versus contrast (TvC) function showed rod threshold decreases as the conditioning pulse contrast increased until ~30% contrast, after which rod threshold increased at the highest rod conditioning pulse contrast (40%) generated within the instrument gamut. A one-way ANOVA found a significant change in threshold as a function of conditioning pulse contrast, $F(1, 3) = 363.60$, $p < 0.001$, with post-hoc analysis identifying

Downloaded from jov.arvojournals.org on 10/03/2022

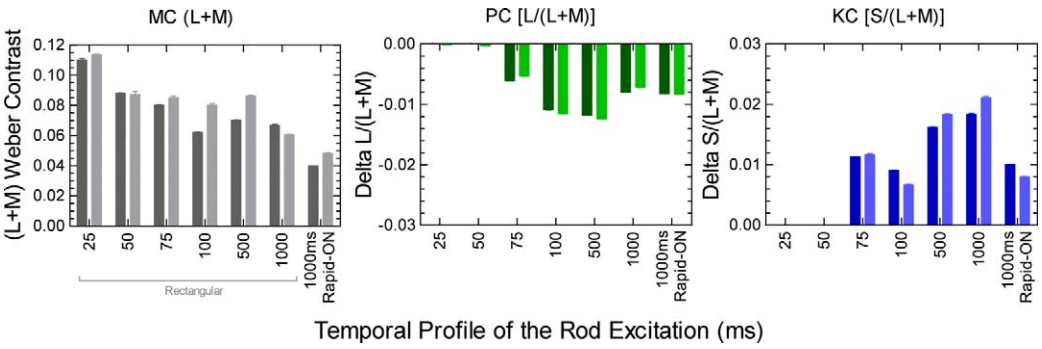

Figure 8. Rod inputs to the three inferred post-receptoral pathways as a function of the temporal profile of the 30% contrast rod signal. The cone excitations ([L+M]; L/[L+M]; S/[L+M]) are shown at the perceptual match to the rod signal for the inferred MC, PC, and KC pathways (left, middle, and right panels, respectively). The data show the mean and standard deviation for observer O_1 (darker colored columns) and observer O_2 (lighter colored columns).

significant differences ($p < 0.001$) in threshold between zero and 10%, 10% and 20%, 20% and 30%, and between 30% and 40% conditioning pulse contrast.

Experiment 2: Post-receptoral pathways mediating the rod signals

Experiment 2 defined the rod inputs to the inferred MC (L+M), PC [L/(L+M)], and KC [S/(L+M)] pathways as a function of the rod signal temporal profile. Figure 8 shows the change in cone excitation ([L+M], L/[L+M], and S/[L+M]) required to match a 30% contrast rod signal. The data ($\mu \pm \sigma$) for observer O_1 are shown in darker colored columns and observer O_2 in lighter colored columns (the data for O_2 are reported in parentheses in the text). The cone excitations at the rod matches were dependent on the rod temporal profile. At the shortest duration measured (25 ms), an 11.0% (11.3%) change in (L+M) was required to match the 30% incremental rod excitation, with no change in L/(L+M) (0.014% change for observer O_2) or S/(L+M) (no change for observer O_2). For the 50 ms duration, an 8.8% (8.7%) change in (L+M) was required, with no change in L/(L+M) (0.027% change for observer O_2) or S/(L+M) (no change for O_2). For durations $\geq$75 ms, a change in (L+M), L/(L+M), and S/(L+M) cone excitations were required for the rod match in both observers. The 75 ms incremental rod excitation was equivalent to an 8.0% (8.5%) increase in (L+M), a 0.6% (0.5%) decrease in L/(L+M), and a 1.1% (1.2%) increase in S/(L+M). In other words, the color appearance of an incremental rod signal of $\geq$75 ms was greenish-blue and brighter. The 100 ms incremental rod excitation was equivalent to a 6.2% (8.0%) increase in (L+M), a 1.1% (1.1%) decrease in L/(L+M), and a 0.8% (0.6%) increase in S/(L+M). The 500 ms incremental rod excitation was equivalent to a 7.0% (8.6%) increase in (L+M), a 1.1% (1.2%) decrease in L/(L+M), and a 1.6% (1.8%) increase in S/(L+M). The 1000 ms incremental rod excitation was equivalent to a 6.6% (6.0%) increase in (L+M), a 0.8% (0.7%) decrease in L/(L+M), and a 1.9% (2.1%) increase in S/(L+M). The 1000 ms rapid-ON rod sawtooth excitation was equivalent to a 4% (4.8%) increase in (L+M), which was 60% (79%) of that required for the 1000 ms rectangular probe, a 0.8% (0.8%) decrease in L/(L+M), similar to that for the rectangular probe, and a 1.0% (0.7%) increase in S/(L+M), which was 54% (38%) of the 1000 ms rectangular probe.

Discussion

The first series of experiments studied the time-course of the temporal adaptation response during interactions between cone photoreceptor signaling, rod and cone photoreceptor signaling, and rod photoreceptor signaling under mesopic illumination using stimulus conditions from which we infer the amplitude and timing of the interaction in the three primary post-receptoral pathways. The SOA paradigm implemented a rapid-ON sawtooth conditioning pulse to favor mediation by the ON-pathway (Cao et al., 2007; Kremers, Lee, Pokorny, & Smith, 1993; Poot et al., 1997) and to study the adaptation response to conditioning pulse onset and subsequent threshold recovery to the steady adaptation level. The cone-cone adaptation response was monophasic for L-cone, LMS, LMSR excitation (Figure 3) and biphasic for +L-M and S-cone excitation stimuli (Figure 4) whereas the rod-rod response to the incremental rod excitation showed a different temporal response compared to cone-cone interactions, indicating that a different process controlled threshold. The difference between the baseline and maximum contrast threshold elevation for the L-

Downloaded from jov.arvojournals.org on 10/03/2022

cone, LMS, LMSR cone-cone photoreceptor interactions were higher than for their rod-cone interaction, and the maximum threshold elevation was delayed by 50 ms in rod-cone interaction condition (Figure 5). There were small or no rod interactions with threshold for the +L-M and S-cone excitation (Figure 6). The second series of experiments observed that the (L+M), L/(L+M), and S/(L+M) cone excitation at the perceptual match to the rod excitation changed with the temporal profile of the rod excitation. We therefore infer that the relative weighting of rod inputs to the MC-, PC-, and KC-pathways depends on the rod temporal profile. We will consider these observations in the following.

Cone-cone interactions

For cone-cone interactions, L-cone, LMS, and LMSR conditions have common monophasic temporal response patterns with maximal threshold elevations at −50 ms SOA and similar average recovery time constants (25 ± 5 ms^{-1}), consistent with the interaction occurring within a common pathway, most likely the nonopponent magnocellular pathway (Cao et al., 2006; Zele et al., 2008). The +L-M and S-cone excitations were chosen to modulate photoreceptor inputs into the inferred PC-pathway and the inferred KC-pathway, with no change in the excitation of the unstimulated photoreceptor classes (Cao et al., 2006; Cao, Zele, et al., 2008; Sun et al., 2001b; Zele et al., 2012). For this low mesopic illumination and rapid-ON sawtooth conditioning pulses, the recovery to baseline was faster (<50 ms) for nonopponent cone signaling than the opponent cone signaling (~500 ms). The few studies measuring the time course of adaptation under dim illuminations with narrow-band chromatic test probe and conditioning pulses all report monophasic response patterns (Adelson, 1982; Buck, 1985; Buck et al., 1984; Frumkes, Sekuler, & Reiss, 1972; von Wiegand et al., 1995; White et al., 1978), and a delayed time to peak of ~50 ms (Adelson, 1982; von Wiegand et al., 1995; White et al., 1978), but none of these test paradigms were designed to measure photoreceptor signaling mediated via the PC-pathway. In this study, the biphasic response for +L-M and S-cone excitations in Figure 4 were phase reversed for the rapid-ON and slow-ON sawtooth conditioning pulses and recovery to baseline threshold following the biphasic response at pulse onset was slower than recovery to baseline for the three nonopponent stimuli (L-cone, LMS and LMSR excitation), with the S-cone excitation condition being slower than the +L-M excitation condition. The recovery time constants are consistent with the slower temporal response of opponent pathways compared to nonopponent pathways, and in particular the KC pathway, as observed in human psychophysics (Krauskopf & Mollon, 1971; Smith, Bowen, & Pokorny, 1984; Swanson et al., 1987).

The biphasic and monophasic adaptation responses may have their origin in the early visual pathways. Recordings from macaque PC-ON cells (+L-M) with a low-frequency (1.22 Hz) rapid-ON sawtooth showed either a peak response to stimulus onset of which was followed by a sustained response that tracked the stimulus ramp profile or a brief cessation in firing with a non-preferred sawtooth stimulus that was followed by a sustained response increase (Kremers et al., 1993). That is, the time-course of the PC-ON (+L-M) cell response histograms showed biphasic response patterns (Kremers et al., 1993) similar to the psychophysical data reported here, and we infer that the biphasic SOA response in Figure 4A may reflect PC-cell activity. By comparison, the macaque MC-ON cells showed either sharp response peaks to the positive transition of a low-frequency rapid-ON sawtooth or a brief cessation in firing to a non-preferred sawtooth stimulus (i.e., rapid-OFF) (Kremers et al., 1993). That is, the time-course of the MC-ON cell response histograms showed monophasic response patterns (Kremers et al., 1993) similar to the L-cone, LMS, and LMSR excitation data (Figure 3). Although the comparable physiological recordings are not available for the KC pathway, we speculate that the biphasic pattern in the S-cone psychophysical data (Figure 4B) might reflect the activity of small bistratified ganglion cells. Because the spatial contrast of the stimuli changed with temporal contrast, further experimentation using spatially larger conditioning pulses will be required to understand the role of the instantaneous level of the conditioning pulse contrast on threshold for the opponent interaction (i.e., the spatial contrast) and to differentiate its role from those changes due to the elapsed time since conditioning pulse onset (i.e., the temporal contrast).

Rod-cone interactions

The rod-cone interaction with the L-cone, LMS, and LMSR excitation condition demonstrated two major differences to the cone-cone interaction data. First, the maximal threshold elevation occurred 50 ms later, at 0 ms SOA, indicating a difference in the temporal response of the cone signals in the MC pathway to the rod conditioning pulse so that rod-cone interactions occur later in time. This delay in the maximum threshold elevation may reflect changes in timing of the cone signal due to rod effects on the temporal impulse response of the cone pathway (Zele et al., 2008) and the temporal lag of the rod signal. Physiological recordings report latency differences between rods and

Downloaded from jov.arvojournals.org on 10/03/2022

cones in the order of 12–20 ms (Schneeweis & Schnapf, 1995; Verweij, Dacey, Peterson, & Buck, 1999) and psychophysical studies of rod and cone signaling mediated via the fast rod pathway indicate rod signal lags of about 8–20 ms for signals mediated via the inferred MC pathway (Cao et al., 2007; Sun et al., 2001b) and by about 40 ms for interactions between rods and S-cone signals mediated via the inferred KC pathway (Zele et al., 2012). The latency differences can increase to between 60 and 80 ms when cone stimulus contrast and/or cone light adaptation is higher (Barbur, 1982; MacLeod, 1972; Sharpe, Stockman, & MacLeod, 1989; van den Berg & Spekreijse, 1977). Second, the amplitude of the L-cone, LMS, and LMSR excitation threshold increase at rod conditioning pulse onset was ~50% lower and has a faster recovery to baseline (36.6 ± 7 ms^{-1}; $\mu \pm SD$) than for the cone-cone interaction condition (25 ± 5 ms^{-1}), likely related to the lower threshold increase for the rod-cone interaction. The implication for cone-mediated mesopic vision is that temporal transients (c.f. a conditioning pulse) activating rods will have a lesser impact on visual sensitivity and recovery will be more rapid than if temporal transients activate only cones. This will be further considered in relation to the results of Experiment 2.

The time-course of peripheral retinal interactions between rod and cone signals have been studied using scotopically or photopically matched narrowband short and long wavelength lights to bias detection to rods or cones (Buck, 1985; Buck et al., 1984; Frumkes et al., 1973; Frumkes et al., 1972). The observations in this study differ from past studies in terms of timing, amplitude, and the pattern of the threshold change during the rod-cone interaction. The timing of the maximum threshold elevation in the cone-cone interaction occurred earlier in time than for the rod-cone interactions in this and the studies by Frumkes et al. (1973, 1972) but that the maximum threshold elevation occurred nearer to conditioning pulse onset in their study and 50 ms prior to conditioning pulse onset in this study (Figure 3). The threshold elevation relative to baseline for the cone-cone data was higher than the threshold change in the rod-cone interaction condition (Figures 3 and 5), whereas Frumkes et al. (1973, 1972) observed similar magnitude threshold elevations for the cone-cone and rod-cone interaction conditions. Notwithstanding the absolute timing differences, this study and their two studies did similarly observe that rod-cone interactions occur later in time than cone-cone interactions. Frumkes et al. (1972) argued that the timing differences reflect the physiologically longer latency of the rod system (Gouras & Link, 1966) such that the rod conditioning pulse causes the maximum threshold elevation to occur later in time than does a cone pulse.

In a study of the time course of the interactions of rod activity on cone signaling (Buck, 1985), scotopic background stimulation (490 nm) rapidly elevated photopic increment thresholds (610 nm) and peak threshold occurred near the time of the onset of the scotopic background, before quickly disappearing (<500 ms) after offset of the 1.5 s scotopic field. This initial transient increase in photopic increment threshold was maintained (sustained) during the scotopic field presentation. Note that the timing of this interaction is similar to the data in Figure 5 and nearer to conditioning pulse onset than the timings observed in the Frumkes studies. Buck (1985) discussed these transient and maintained interactions in terms of a simple center-surround model to explain the transitory interaction as manifestation of a longer latency of the antagonistic surround mechanism as compared to the center mechanisms. In his model, the nearby scotopic excitation raises photopic threshold and more distant scotopic stimulation antagonized the interaction. Although useful as a model of spatial properties of the rod and cone photoreceptor interactions and the time course of the rod threshold changes during cone activation (Buck et al., 1984), the transitory interaction appeared to be spatially independent of the test field size and so is not fully explained by the center-surround model (Buck, 1985). We explored the effect of a spatially larger rod adapting conditioning pulse on the rod threshold and found that the threshold pattern was similar for both the larger and spatially coextensive rod conditioning fields (unfilled squares and circles in Figure 7A). Given that Buck (1985) observed that transient interactions were independent of test field size and that our data showed a similar relationship, then it follows that the rapid-ON sawtooth may be exposing a similar transient interaction. The development of future models of the transient interaction will need to explain additional factors, including the effect of illumination level rather than wavelength for modulating the relative levels of rod and cone activity inside and outside the stimulus area (lateral rod-cone interaction) (Zele & Vingrys, 2007), and recent evidence that the rate of adaptation during rod-cone interaction varies with retinal eccentricity (this study was conducted at 7° eccentricity), with greater speed for retinal areas between 6° and 9° than for the fovea or eccentricities beyond 9° (Matesanz et al., 2011).

The analysis of the rod signal interactions with the +L-M and S-cone excitation showed no significant interactions for one observer while the second observer showed a facilitatory interaction between the rod stimulus and +L-M and S-cone stimuli. The literature identifies a number of potential loci for the facilitatory interactions. Rod effects on chromatic discrimination indicate that rod signaling in the MC pathway can subserve interactions with S-cone signals (Cao, Zele, et

Downloaded from jov.arvojournals.org on 10/03/2022

al., 2008) and linear interactions of rod and S-cone signals within the KC-pathway produce supra-additivity of the combined rod and S-cone thresholds (Zele et al., 2012), but such interactions can be small or absent in some observers (Zele et al., 2012). When cone signals are mediated via the PC pathway, the rod and cone signals can show probability summation, indicating that signaling is mediated via different post-receptoral pathways (Sun et al., 2001b) and there is also interindividual variation (Sun et al., 2001b). The study of rod effects on unique hue settings (Buck et al., 1998; Buck, Knight, & Bechtold, 2000; Buck, Thomas, Connor, Green, & Quintana, 2008; Nerger, Volbrecht, & Ayde, 1995) has also been used to infer the post-receptoral opponent pathways mediating rod signals. In an analysis of the time-course of the rod hue biases on unique hues, Buck et al. (2008) demonstrated that changes in the red-green balance at unique yellow, which is inferred mediation by the PC-pathway, can occur in less than 20 ms. By comparison, the time course of the changes in red-green balance at unique blue, which is inferred mediation by the KC-pathway, had a latency of less than 100 ms (Buck et al., 2008). Although the methodologies of this and the unique hue studies of rod signaling in opponent pathways are different, and the results of both approaches show individual differences that are still to be explored, there were commonalities in the timing estimates; the maximal threshold change for the interaction between the rod and +L-M signals for observer O_2 in Figure 6 occurred at about 50 ms (the 50 ms rod signal required a 0.027% change in L/(L+M); Figure 8), and the rod interaction with the rod and S-cone signal occurred by 100 ms (a 75 ms rod signal required a 1.16% change in S/(L+M), and a 100 ms rod signal required a 0.66% change; Figure 8).

Rod-rod interactions

The rod-rod interaction (Figure 6) showed a decrease in threshold for the incremental rod excitation measured during the rod conditioning pulse presentation with a slow recovery time constant (0.7 ± 0.2 ms^{-1}) that returned to baseline thresholds in ~1000 ms. The timing of the maximum threshold change for the rod-rod interaction data was between 0 ms and 100 ms after conditioning pulse onset (Figure 6) in the range reported by Frumkes et al. (1973, 1972), but importantly, the rod threshold was lower than the baseline threshold during the presentation of the rod conditioning pulse in this study (sensitized in their terminology) and elevated (desensitized) in their study. We infer from the color matching data (Figure 8) that the 25 ms incremental rod test probe was mediated solely via the MC pathway, whereas the 1000 ms rod rapid-ON conditioning pulse excitation produced differential activations of the MC, PC, and KC pathways. The threshold decrease was contrast dependent such that a rod conditioning pulse signal facilitated rod detection at low contrasts and increased rod threshold at higher contrasts, producing a shape characteristic of the dipper-shaped threshold versus contrast (TvC) function for luminance pedestals (Anderson & Vingrys, 2000; Boynton & Foley, 1999; Cornsweet & Pinsker, 1965; Whittle & Swanston, 1974; Zele & Vingrys, 2007). Thirty percent rod contrast produced the maximum rod facilitation with these experimental conditions. The monophasic response pattern for the decrement in rod excitation (Figure 7A, filled symbols) showed a threshold increase during the conditioning pulse and a rapid recovery to baseline, more similar to the cone-cone data (Figure 3). That the data are not dependent on the spatial extent of the rod conditioning pulse indicates the rod-rod summation is a local area effect. We conjecture that the improvement in incremental rod sensitivity during the conditioning pulse presentation is due to the summation of the rod test probe and rod conditioning pulse. Given that under the 5 Td mesopic illumination, rod signals are likely transmitted via gap junctions to cone pedicles and mediated via cone pathways to the visual cortex, the threshold increase during cone-cone interactions and the threshold decrease during rod-rod interactions (Figures 3 and 7) point to some intrinsic property of the different neurons in the different post-receptoral pathways acting on rod and cone signals that causes the rod signals to be processed differently, including both the amplitude and with what temporal response they affect the post-receptoral pathways.

Post-receptoral pathways mediating the rod signals

The second experiment demonstrated that rod contributions to the MC, PC, and KC post-receptoral pathways were dependent on the temporal profile (duration and waveform) of the input signal (Figure 8). The (L+M) luminance contrast change at the rod color match was largest at all probe durations and we infer that rod contributions were strongest in the MC pathway for all rod temporal profiles. For probe durations of 75 ms and longer, the chromaticity of the rod color match was consistent with activity in the inferred MC, PC, and KC pathways in both observers. This finding extends previous observations where rod activity was shown to generate chromaticity shifts in directions other than towards white under mesopic illumination with 1 Hz (500 ms ON, 500 ms OFF periods) stimuli (Cao et al., 2005), and with increasing exposure time under scotopic conditions (Stabell &

Downloaded from jov.arvojournals.org on 10/03/2022

Stabell, 1999), consistent with the present observation for rod contributions to cone opponent pathways with durations longer than about 75 ms.

The rapid-ON sawtooth stimulus initiated a similar response to rectangular stimuli of the same duration within the PC pathway, however input to the KC pathway was ~50% less, and the MC pathway was ~40% less, indicating a difference in the temporal filtering of the opponent and nonopponent pathways to the rod signal. This observation also has implications for the interpretation of SOA experiments. Based on the contrast of the cone excitations that matched the rod signal (Figure 8), we infer that the larger threshold loss for the cone-cone interaction (Figure 3) compared to the rod-cone interaction data (Figure 5) reflects the difference in the relative strength of the rod and cone signals in the three pathways. If we assume that cells in the MC, PC, and KC pathways show linear relationships between response and stimulus contrast for the conditions of this experiment, as Purpura, Kaplan, and Shapley (1988) have reported for their physiological recordings in macaque PC and MC cells at mesopic illuminations <30 Td, and Cao, Pokorny, Smith and Zele (2008) have shown in their psychophysical analysis of rod contributions to the inferred MC, PC, and KC pathways, then it follows from Figure 8 that the L+M cell responses to a 30% L+M contrast signal during the cone-cone interaction (Figure 3) will be larger than their response to a 30% rod signal (Figure 5), consistent with a higher threshold in the cone-cone interactions. Taken together, the change in timing of the maximum threshold elevation in the cone-cone and rod-cone interactions could reflect differences in the post-receptoral temporal filtering of rod and cone signals and the slower temporal response of rod photoreceptors, with the change in relative weighting of rod signals within the three primary post-receptoral pathways contributing to the differences in the amplitude of the photoreceptor interactions.

Comment

The relative sensitivities and temporal responses of rod and cone mediated mesopic vision depend on complex interactions between the photoreceptor and post-receptoral pathway sensitivities to the temporal, spatial, and viewing eccentricity of the lights, the adapting illumination level, and stimulus chromaticities. Many of these dependencies and their effects of mesopic vision remain largely unexplored. For the conditions examined in this experiment, the rapid-ON sawtooth stimulus quantified the time course of the transient mechanism without intrusion of the sustained photoreceptor interaction, nor interactions between ON- and OFF-pathways that can occur with rectangular stimuli. The clear differences in timing and threshold amplitudes observed in this study and those observed in past studies are likely to include differences in experimental methodology. An example is that a wavelength and/or illumination level that biases activity to rods or cones can introduce illumination dependent changes in photoreceptor time constants and sensitivity variations to stimulus chromaticities that affect the timing and threshold amplitudes of the measured interactions. The four-primary colorimeter starts at the same chromaticity and illumination level for all conditions so as to adapt the four photoreceptor classes to an equal energy spectrum. In the relative cone Troland chromaticity space, the SMLR photoreceptor excitations at the equal energy spectrum were equal to 5, 1.667, 3.333, and 5 Td, respectively. During presentation of the test probe and conditioning pulse, the four-primary colorimeter independently controlled the degree of excitation of the rods and three cone photoreceptor classes and their inputs to the inferred post-receptoral pathways by changing one or a combination of photoreceptor excitations, therefore allowing direct measurement of interaction under the same experimental conditions. This lends to more direct inferences about the nature of the timing and amplitude changes in the inferred physiological substrates mediating the interactions.

This study demonstrates, for the temporal, spatial, and illumination levels measured, that the time course of mesopic visual adaptation has different time constants, amplitudes, and threshold response patterns for the different photoreceptor classes and interaction types. We infer that that the amplitudes of the rod-cone interactions could vary depending on the rod signal strength in the post-receptoral pathways mediating the cone signals, with the temporal profile of the rod signal affecting the relative rod-signal strength in the pathways. This points to some yet to be defined intrinsic differences within the post-receptoral pathways that result in the differential processing of the rod and cone signals. For vision, we speculate that the rapid time-course of the interactions under mesopic illumination could serve a useful purpose by minimizing transient sensitivity losses when light onset activates both rods and cones, and this could be accomplished by transmitting rod signals through multiple post-receptoral pathways.

Acknowledgments

Australian Research Council Discovery Project ARC-DP1096354 (AJZ) supported this research. We

Downloaded from jov.arvojournals.org on 10/03/2022

thank Aaron A'brook for technical assistance in software development.

Commercial relationships: none.
Corresponding author: Andrew J. Zele.
Email: andrew.zele@qut.edu.au.
Address: Institute of Health and Biomedical Innovation and School of Optometry and Vision Science, Queensland University of Technology, Brisbane, Australia.

References

Adelson, E. H. (1982). Saturation and adaptation in the rod system. *Vision Research*, *22*(10), 1299–1312.

Anderson, A. J., & Vingrys, A. J. (2000). Interactions between flicker thresholds and luminance pedestals. *Vision Research*, *40*(19), 2579–2588.

Baker, H. D. (1953). The instantaneous threshold and early dark adaptation. *Journal of the Optical Society of America*, *43*(9), 798–803.

Barbur, J. L. (1982). Reaction-time determination of the latency between visual signals generated by rods and cones. *Ophthalmic and Physiological Optics*, *2*(3), 179–185.

Barbur, J. L., & Konstantakopoulou, E. (2012). Changes in color vision with decreasing light level: Separating the effects of normal aging from disease. *Journal of the Optical Society of America, 29*(2), A27–A35.

Bowen, R. W., Markell, K. A., & Schoon, C. M. (1980). Two-pulse discrimination and rapid light adaptation: Complex effects on temporal resolution and a new visual temporal illusion. *Journal of the Optical Society of America, 70*(12), 1453–1458.

Boynton, G. M., & Foley, J. M. (1999). Temporal sensitivity of human luminance pattern mechanisms determined by masking with temporally modulated stimuli. *Vision Research*, *39*(9), 1641–1656.

Boynton, R. M., Bush, W. R., & Enoch, J. M. (1954). Rapid changes in foveal sensitivity resulting from direct and indirect adapting stimuli. *Journal of the Optical Society of America*, *44*(1), 56–60.

Buck, S. L. (1985). Cone-rod interaction over time and space. *Vision Research*, *25*(7), 907–916.

Buck, S. L. (2004). Rod-cone interactions in human vision. In L. M. Chalupa & J. S. Werner (Eds.), *The visual neurosciences* (Vol. 1, pp. 863–878). Massachusetts: The MIT Press.

Buck, S. L., Juve, R., Wisner, D., & Concepcion, A. (2012). Rod hue biases produced on CRT displays. *Journal of the Optical Society of America*, *29*(2), A36–A43.

Buck, S. L., Knight, R., Fowler, G., & Hunt, B. (1998). Rod influence on hue-scaling functions. *Vision Research*, *38*(21), 3259–3263.

Buck, S. L., Knight, R. F., & Bechtold, J. (2000). Opponent-color models and the influence of rod signals on the loci of unique hues. *Vision Research*, *40*(24), 3333–3344.

Buck, S. L., Stefurak, D. L., Moss, C., & Regal, D. (1984). The time-course of rod-cone interaction. *Vision Research*, *24*(6), 543–548.

Buck, S. L., Thomas, L. P., Connor, C. R., Green, K. B., & Quintana, T. (2008). Time course of rod influences on hue perception. *Visual Neuroscience*, *25*(3), 517–520.

Cao, D., Lee, B. B., & Sun, H. (2010). Combination of rod and cone inputs in parasol ganglion cells of the magnocellular pathway. *Journal of Vision*, *10*(11):4 1–15, http://www.journalofvision.org/content/10/11/4, doi:10.1167/10.11.4. [PubMed] [Article]

Cao, D., & Lu, Y. H. (2012). Lateral suppression of mesopic rod and cone flicker detection. *Journal of the Optical Society of America*, *29*(2), A188–A193.

Cao, D., Pokorny, J., & Smith, V. C. (2005). Matching rod percepts with cone stimuli. *Vision Research*, *45*(16), 2119–2128.

Cao, D., Pokorny, J., Smith, V. C., & Zele, A. J. (2008). Rod contributions to color perception: Linear with rod contrast. *Vision Research, 48*(26), 2586–2592.

Cao, D., Zele, A. J., & Pokorny, J. (2006). Dark-adapted rod suppression of cone flicker detection: Evaluation of receptoral and postreceptoral interactions. *Visual Neuroscience*, *23*(3-4), 531–537.

Cao, D., Zele, A. J., & Pokorny, J. (2007). Linking impulse response functions to reaction time: Rod and cone reaction time data and a computational model. *Vision Research, 47*(8), 1060–1074.

Cao, D., Zele, A. J., & Pokorny, J. (2008). Chromatic discrimination in the presence of incremental and decremental rod pedestals. *Visual Neuroscience*, *25*(3), 399–404.

CIE. (1964). *CIE proceedings (Committee report E-1.4.1)*. Paper presented at the CIE Proceedings, Vienna.

Cornsweet, T. N., & Pinsker, H. M. (1965). Luminance discrimination of brief flashes under various conditions of adaptation. *The Journal of Physiology, 176,* 294–310.

Crawford, B. H. (1947). Visual adaptation in relation

Downloaded from jov.arvojournals.org on 10/03/2022

to brief conditioning stimuli. *Proceedings of the Royal Society of London*, *134*(875), 283–302.

Crook, J. D., Davenport, C. M., Peterson, B. B., Packer, O. S., Detwiler, P. B., & Dacey, D. M. (2009). Parallel ON and OFF cone bipolar inputs establish spatially coextensive receptive field structure of blue-yellow ganglion cells in primate retina. *The Journal of Neuroscience*, *29*(26), 8372–8387.

Daw, N. W., Jensen, R. J., & Brunken, W. J. (1990). Rod pathways in mammalian retinae. *Trends in Neurosciences*, *13*(3), 110–115.

Feigl, B., Cao, D., Morris, C. P., & Zele, A. J. (2011). Persons with age-related maculopathy risk genotypes and clinically normal eyes have reduced mesopic vision. *Investigative Ophthalmology & Visual Science*, *52*(2), 1145–1150, http://www.iovs.org/content/52/2/1145. [PubMed] [Article]

Field, G. D., Greschner, M., Gauthier, J. L., Rangel, C., Shlens, J., Sher, A. et al. (2009). High-sensitivity rod photoreceptor input to the blue-yellow color opponent pathway in macaque retina. *Nature Neuroscience, 12*(9), 1159–1164.

Frumkes, T. E., Sekuler, M. D., Barris, M. C., Reiss, E. H., & Chalupa, L. M. (1973). Rod-cone interaction in human scotopic vision. I. Temporal analysis. *Vision Research*, *13*(7), 1269–1282.

Frumkes, T. E., Sekuler, M. D., & Reiss, E. H. (1972). Rod-cone interaction in human scotopic vision. *Science*, *175*(4024), 913–914.

Goldberg, S. H., Frumkes, T. E., & Nygaard, R. W. (1983). Inhibitory influence of unstimulated rods in the human retina: Evidence provided by examining cone flicker. *Science, 221*(4606), 180–182.

Gouras, P., & Link, K. (1966). Rod and cone interaction in dark-adapted monkey ganglion cells. *The Journal of Physiology*, *184*(2), 499–510.

Graham, N., & Hood, D. C. (1992). Modeling the dynamics of light adaptation: The merging of two traditions. *Vision Research, 32*(7), 1373–1393.

Hayhoe, M. M., Benimoff, N. I., & Hood, D. C. (1987). The time-course of multiplicative and subtractive adaptation process. *Vision Research*, *27*(11), 1981–1996.

Hecht, S. (1920). Human retinal adaptation. *Proceedings of the National Academy of Sciences*, *6*(3), 112–115.

Hecht, S., Haig, C., & Chase, A. M. (1937). The influence of light adaptation on subsequent dark adaptation of the eye. *The Journal of General Physiology*, *20*(6), 831–850.

Hood, D. C., & Finkelstein, M. A. (1986). Sensitivity to light. In K. R. Boff, L. Kaufamn, & J. P. Thomas (Eds.), *Handbook of perception and human performance* (Vol. 1, pp. 1–66). New York: Wiley.

Hood, D. C., Ilves, T., Maurer, E., Wandell, B., & Buckingham, E. (1978). Human cone saturation as a function of ambient intensity: A test of models of shifts in the dynamic range. *Vision Research, 18*(8), 983–993.

Kohn, A. (2007). Visual adaptation: Physiology, mechanisms, and functional benefits. *Journal of Neurophysiology, 97*(5), 3155–3164.

Kolb, H., & Famiglietti, E. V. (1974). Rod and cone pathways in the inner plexiform layer of cat retina. *Science*, *186*(4158), 47–49.

Krauskopf, J., & Mollon, J. D. (1971). The independence of the temporal integration properties of individual chromatic mechanisms in the human eye. *The Journal of Physiology*, *219*(3), 611–623.

Kremers, J., Lee, B. B., Pokorny, J., & Smith, V. C. (1993). Responses of macaque ganglion cells and human observers to compound periodic waveforms. *Vision Research*, *33*(14), 1997–2011.

Kremers, J., & Meierkord, S. (1999). Rod-cone-interactions in deuteranopic observers: Models and dynamics. *Vision Research*, *39*(20), 3372–3385.

Lee, B. B., Martin, P. R., & Grünert, U. (2010). Retinal connectivity and primate vision. *Progress in Retinal and Eye Research*, *29*(6), 622–639.

Lee, B. B., Pokorny, J., Smith, V. C., Martin, P. R., & Valberg, A. (1990). Luminance and chromatic modulation sensitivity of macaque ganglion cells and human observers. *Journal of the Optical Society of America A*, *7*(12), 2223–2236.

Lee, B. B., Smith, V. C., Pokorny, J., & Kremers, J. (1997). Rod inputs to macaque ganglion cells. *Vision Research*, *37*(20), 2813–2828.

Li, W., Chen, S., & DeVries, S. H. (2010). A fast rod photoreceptor signaling pathway in the mammalian retina. *Nature Neuroscience*, *13*(4), 414–416.

Lie, I. (1963). Dark adaptation and the photochromatic interval. *Documenta Ophthalmologica, 17,* 411–510.

Limb, J. O., & Tulunay-Keesey, U. (1981). Spatiotemporal characteristics of thresholds adjacent to a luminance edge. *Journal of the Optical Society of America*, *11*(10), 1209–1219.

MacLeod, D. I. (1972). Rods cancel cones in flicker. *Nature*, *235*(5334), 173–174.

MacLeod, D. I., & Boynton, R. M. (1979). Chromaticity diagram showing cone excitation by stimuli of equal luminance. *Journal of the Optical Society of America*, *69*(8), 1183–1186.

Matesanz, B. M., Issolio, L., Arranz, I., de la Rosa, C.,

Downloaded from jov.arvojournals.org on 10/03/2022

Menéndez, J. A., Mar, S. et al. (2011). Temporal retinal sensitivity in mesopic adaptation. *Ophthalmic and physiological optics*, *31*(6), 615–624.

Müller, G. E. (1923). Zur Theorie des Stäbchenapparates und der Zapfenblindheit (On the theory of rod and cone monochromacy). *Zeitschrift für Psychologie und Physiologie der Sinnesorgane, 54,* 9–48 & 102–145.

Nagel, W. (1911). Adaptation, twilight vision, and the duplicity theory. In A. Gullstrand, J. von Kries, & W. Nagel (Eds.), *Handbuch der physiologischen optik von H. von Helmholtz*. (pp. 313–394). Hamburg and Leipzig: Leopold Voss.

Nagel, W. (1924). Adaptation, twilight vision, and the duplicity theory. In A. Gullstrand, J. von Kries, & W. Nagel (Eds.), *Handbuch der physiologischen optik von H. von Helmholtz*. (pp. 313–394). Hamburg and Leipzig: Leopold Voss.

Nemes, V. A., Parry, N. R. A., & McKeefry, D. J. (2010). A behavioural investigation of human visual short term memory for colour. *Ophthalmic and Physiological Optics*, *30*(5), 594–601.

Nerger, J. L., Volbrecht, V. J., & Ayde, C. J. (1995). Unique hue judgments as a function of test size in the fovea and at 20-deg temporal eccentricity. *Journal of the Optical Society of America*, *12*(6), 1225–1232.

Pokorny, J., Lutze, M., Cao, D., & Zele, A. J. (2006). The color of night: Surface color perception under dim illuminations. *Visual Neuroscience*, *23*(3-4), 525–530.

Pokorny, J., Smithson, H., & Quinlan, J. (2004). Photostimulator allowing independent control of rods and the three cone types. *Visual Neuroscience*, *21*(3), 263–267.

Pokorny, J., Sun, V. C. W., & Smith, V. C. (2003). Temporal dynamics of early light adaptation. *Journal of Vision, 3*(6):3, 423–431, http://www.journalofvision.org/content/3/6/3, doi:10.1167/3.6.3. [PubMed] [Article]

Polyak, S. L. (1948). *The retina*. Chicago: University of Chicago Press.

Poot, L., Snippe, H. P., & van Hateren, J. H. (1997). Dynamics of adaptation at high luminances: Adaptation is faster after luminance decrements than after luminance increments. *Journal of the Optical Society of America. 14*(9), 2499–2508.

Purpura, K., Kaplan, E., & Shapley, R. M. (1988). Background light and the contrast gain of primate P and M retinal ganglion cells. *Proceedings of the National Academy of Sciences of the United States of America*, *85*(12), 4534–4537.

Purpura, K., Tranchina, D., Kaplan, E., & Shapley, R. M. (1990). Light adaptation in the primate retina: Analysis of changes in gain and dynamics of monkey retinal ganglion cells. *Visual Neuroscience, 4*(1), 75–93.

Puts, M. J. H., Pokorny, J., Quinlan, J., & Glennie, L. (2005). Audiophile hardware in vision science; The soundcard as a digital to analog converter. *Journal of Neuroscience Methods, 142*(1), 77–81.

Rucci, M., & Beck, J. (2005). Effects of ISI and flash duration on the identification of briefly flashed stimuli. *Spatial Vision*, *18*(2), 259–273.

Schneeweis, D. M., & Schnapf, J. L. (1995). Photovoltage of rods and cones in the macaque retina. *Science*, *268*(5213), 1053–1056.

Schultze, M. (1866). Zur Anatomie und Physiologie der Retina (On the anatomy and physiology of the retina). *Archiv für mikroskopische Anatomie, 2,* 175–286.

Shapiro, A. G., Pokorny, J., & Smith, V. C. (1996). Cone-rod receptor spaces with illustrations that use CRT phosphor and light-emitting-diode spectra. *Journal of the Optical Society of America*, *13*(12), 2319–2328.

Sharpe, L. T., Stockman, A., & MacLeod, D. I. (1989). Rod flicker perception: Scotopic duality, phase lags and destructive interference. *Vision Research, 29*(11), 1539–1559.

Smith, V. C., Bowen, R. W., & Pokorny, J. (1984). Threshold temporal integration of chromatic stimuli. *Vision Research*, *24*(7), 653–660.

Smith, V. C., & Pokorny, J. (1975). Spectral sensitivity of the foveal cone photopigments between 400 and 500 nm. *Vision Research*, *15*(2), 161–171.

Smith, V. C., & Pokorny, J. (1996). The design and use of a cone chromaticity space: A tutorial. *Color Research and Application*, *21*(5), 375–383.

Smith, V. C., Pokorny, J., Lee, B. B., & Dacey, D. M. (2008). Sequential processing in vision: The interaction of sensitivity regulation and temporal dynamics. *Vision Research*, *48*(26), 2649–2656.

Stabell, U., & Stabell, B. (1971). Chromatic rod vision. II. Wavelength of pre-stimulation varied. *Scandinavian Journal of Psychology*, *12*(4), 282–288.

Stabell, U., & Stabell, B. (1999). Rod-cone color mixture: Effect of size and exposure time. *Journal of the Optical Society of America, 16*(11), 2638–2642.

Stiles, W. S. (1978). *Mechanisms of colour vision*. London: Academic Press Inc.

Stockman, A., Langendörfer, M., Smithson, H. E., &

Downloaded from jov.arvojournals.org on 10/03/2022

Sharpe, L. T. (2006). Human cone light adaptation: From behavioral measurements to molecular mechanisms. *Journal of Vision, 6*(11):5, 1194–1213, http://www.journalofvision.org/content/6/11/5, doi:10.1167/6.11.5. [PubMed] [Article]

Sun, H., Pokorny, J., & Smith, V. C. (2001a). Brightness induction from rods. *Journal of Vision, 1*(1):4, 32–41, http://www.journalofvision.org/content/1/1/4, doi:10.1167/1.1.4. [PubMed] [Article]

Sun, H., Pokorny, J., & Smith, V. C. (2001b). Rod-cone interactions assessed in inferred magnocellular and parvocellular postreceptoral pathways. *Journal of Vision, 1*(1):5, 42–54, http://www.journalofvision.org/content/1/1/5, doi:10.1167/1.1.5. [PubMed] [Article]

Swanson, W. H., Ueno, T., Smith, V. C., & Pokorny, J. (1987). Temporal modulation sensitivity and pulse-detection thresholds for chromatic and luminance perturbations. *Journal of the Optical Society of America A*, *4*(10), 1992–2005.

Swanson, W. H., Pan, F., & Lee, B. B. (2008). Chromatic temporal integration and retinal eccentricity: Psychophysics, neurometric analysis and cortical pooling. *Vision Research, 48*(26), 2657–2662.

Trezona, P. W. (1970). Rod participation in the 'blue' mechanism and its effect on colour matching. *Vision Research*, *10*(4), 317–332.

van den Berg, T. J., & Spekreijse, H. (1977). Interaction between rod and cone signals studied with temporal sine wave stimulation. *Journal of the Optical Society of America*, *67*(9), 1210–1217.

Verweij, J., Dacey, D. M., Peterson, B. B., & Buck, S. L. (1999). Sensitivity and dynamics of rod signals in H1 horizontal cells of the macaque monkey retina. *Vision Research*, *39*(22), 3662–3672.

Virsu, V., & Lee, B. B. (1983). Light adaptation in cells of macaque lateral geniculate nucleus and its relation to human light adaptation. *Journal of Neurophysiology*, *50*(4), 864–878.

Virsu, V., Lee, B. B., & Creutzfeldt, O. D. (1977). Dark adaptation and receptive field organisation of cells in the cat lateral geniculate nucleus. *Experimental Brain Research*, *27*(1), 35–50.

von Kries, J. (1929). Zur Theorie des Tages und Dämmerungssehens (On the theory of hemeralopia and nyctalopia). In A. Bethe, G. Bergmann, G. Embden & A. Ellinger (Eds.), *Handbuch der normalen und pathologischen Physiologie*. (pp. 679–713). Berlin: Springer.

von Wiegand, T. E., Hood, D. C., & Graham, N. (1995). Testing a computational model of light-adaptation dynamics. *Vision Research*, *35*(21), 3037–3051.

Weiss, S., Kremers, J., & Maurer, J. (1998). Interaction between rod and cone signals in responses of lateral geniculate neurons in dichromatic marmosets (Callithrix jacchus). *Visual Neuroscience*, *15*(5), 931–943.

White, T. W., Kelly, S. A., & Sturr, J. F. (1978). Large field early light adaptation. *Vision Research*, *18*(12), 1679–1684.

Whittle, P., & Swanston, M. T. (1974). Luminance discrimination of separated flashes: The effect of background luminance and the shapes of T.V.I. curves. *Vision Research, 14*(8), 713–719.

Wiesel, T. N., & Hubel, D. H. (1966). Spatial and chromatic interactions in the lateral geniculate body of the rhesus monkey. *Journal of Neurophysiology*, *29*(6), 1115–1156.

Willmer, E. N. (1950). Low threshold rods and the perception of blue. *Journal of Physiology,* (11), 17.

Zele, A. J., Cao, D., & Pokorny, J. (2008). Rod-cone interactions and the temporal impulse response of the cone pathway. *Vision Research*, *48*(26), 2593–2598.

Zele, A. J., Kremers, J., & Feigl, B. (2012). Mesopic rod and S-cone interactions revealed by modulation thresholds. *Journal of the Optical Society of America*, *29*(2), A19–A26.

Zele, A. J., & Vingrys, A. J. (2000). Flicker adaptation can be explained by probability summation between ON- and OFF-mechanisms. *Clinical & Experimental Ophthalmology*, *28*(3), 227–229.

Zele, A. J., & Vingrys, A. J. (2007). Defining the detection mechanisms for symmetric and rectified flicker stimuli. *Vision Research*, *47*(21), 2700–2713.

Downloaded from jov.arvojournals.org on 10/03/2022